Available online at www.sciencedirect.com
ScienceDirect
Journal of Nuclear Materials 375 (2008) 65–71
journal of nuclear materials
www.elsevier.com/locate/jnucmat

Correlation between composition of passive layer and corrosion behavior of high Si-containing austenitic stainless steels in nitric acid

R. Robin[a,*], F. Miserque[b], V. Spagnol[a]

[a] *CEA Saclay, DEN/DANS/DPC/SCCME, Bât. 458, 91191 Gif sur Yvette, France*
[b] *CEA Saclay, DEN/DANS/DPC/SCP, Bât. 391, 91191 Gif sur Yvette, France*

Received 25 January 2007; accepted 31 October 2007

Abstract

Austenitic stainless steels with 18% Cr have a good corrosion behavior in pure nitric acid. However, when oxidizing power of the solution increases, this kind of stainless steels faces a severe intergranular corrosion. Adding a sufficiently high concentration of silicon to the steel avoids this type of corrosion: in oxidizing solutions, those stainless steels exhibit generalized corrosion but their dissolution rate is higher than the one of stainless steels without silicon. To find out the role of silicon on such effects, the corrosion behavior of two different stainless steels with equivalent chromium content but with different silicon content (304L steel and Uranus S1N) has been studied in concentrated nitric acid solutions. Correlations have been evidenced between the passive layer composition investigated by XPS analysis and the corrosion behavior characterized by electrochemical techniques. The presence of silicon in the steel changes neither the oxidation state of chromium or iron, nor the ratio between iron and chromium in the passive layer. Silicon is present in the passive layer in an important content (35 at.%) and thus decreases the chromium content of the passive layer (80 and 50 at.% respectively for 304L steel and Uranus S1N after nitric passivation). Uranus S1N exhibits a less protective passive layer and so its generalized corrosion rate is higher than the one of 304L steel. A selective deposition of platinoïds highlights differences of polarization distribution on the surface between the grain boundaries and grain faces for theses steels. For Uranus S1N, the similar electrochemical behavior of grain boundaries and faces might be connected with the homogeneous silicon distribution.

© 2007 Elsevier B.V. All rights reserved.

1. Introduction

Austenitic stainless steels are largely used as structural materials for equipments handling nitric acid media. The corrosion resistance of stainless steels depends on the spontaneous formation of a protective surface layer. This passive film is usually very thin (about 1–10 nm thick) and Cr is concentrated in the film [1,2]. The corrosion resistance is maintained by the protective effect of Cr^{III} oxide and Cr^{III} oxyhydroxide film [3], thermodynamically stable in nitric acid environments. However, when exposed to strongly oxidizing nitric acid media (concentrated nitric acid, presence of oxidizing species...), these steels are susceptible to severe intergranular corrosion, even if the steels are not sensitized. The corrosion potential of these steels is shifted towards their transpassive domain, and the passive film is dissolved, especially by oxidation of Cr^{III} into Cr^{VI} [4–6], which is soluble in nitric acid solution.

Silicon is known as one of the most important alloying elements introduced in austenitic stainless steels to increase their corrosion resistance in strongly oxidizing nitric acid environments, and specially to inhibit the intergranular corrosion. However, the susceptibility of silicon-containing stainless steels to intergranular corrosion depends on the concentration of silicon and its distribution in the steel, as well as on the conditions and composition of the corrosive environment [5,7–11]. For example, in boiling HNO_3

---

[*] Corresponding author.
E-mail address: rapheal.robin@cea.fr (R. Robin).

0022-3115/$ - see front matter © 2007 Elsevier B.V. All rights reserved.
doi:10.1016/j.jnucmat.2007.10.016

containing oxidizing species (i.e. Coriou solution: Cr^{VI}), silicon additions in the steel (>2 wt%) decrease the weight loss rate by eliminating the intergranular attacks. By contrast, in pure HNO_3 (i.e. Huey solution), the corrosion rate increases continuously with the Si-content of the steels [7,8,10].

The beneficial influence of Si on the corrosion resistance of stainless steels in strongly oxidizing nitric acid media is usually related to the formation of protective oxide films enriched in silicon oxide SiO_2. Si-oxide is formed under potential inside the transpassive regions and suppresses the cathodic reaction, and consequently decreases the corrosion rate [5,7,9,10]. In passive potential regions, the passive film is mainly composed of Cr oxide, and Si additions in the steel reduce the corrosion resistance as the Cr concentration in the film decreases. However this hypothesis remains questionable and does not explain intergranular corrosion susceptibility. Several authors support the idea that the segregation of Si at grain boundaries is responsible for the intergranular corrosion susceptibility. According to Ghiban [12], for high Si containing stainless steels, the intergranulary segregated silicon allows to avoid the chromium carbide formation (carbon preferably segregates in matrix), and consequently the selective dissolution of chromium depleted zones which causes intergranular corrosion. Kasparova [11] takes into account the changes in the electronic structure of grain boundaries under the effect of the intergranularly segregated silicon which is more electronegative than the basic metallic components of the steel, and consequently affects the chemisorption process of the ionic components of the solution at the grain boundaries.

Although Si is an effective alloying element in stainless steels, the relationship between the surface film and the corrosion resistance of the high Si-containing stainless steels used in nitric acid is not clear and the influence of silicon remains ambiguous. Based on X-ray photoelectron spectroscopy (XPS) analyses and anodic polarization at constant potential, the aim of the study presented here is to investigate the composition of passive films of high Si-containing austenitic stainless steels in nitric acid environments. This preliminary work is focused on:

- The relationship between the composition of the passive films and the corrosion behavior of stainless steels for different electrochemical states (from passive to transpassive state);
- the chemical form of silicon in the passive films;
- a specific experiment to highlight the polarization distributions on the surface between grain boundaries and grain faces of high and low Si-containing steels.

To find out the role of silicon, two different stainless steels with equivalent chromium content but with different silicon content will be studied.

2. Experimental procedures

2.1. Material and surface specimen preparation

The chemical composition of the commercial stainless steels used is given in Table 1. The two steels are AISI 304L SS (Z2 CN 18-10) and Uranus S1N (Z1 CNS 18-15). They have the same chromium content (18 wt%) but different silicon content, about 0.4 wt% and 4 wt%, respectively for 304L SS and Uranus S1N. These steels are not sensitized and have a low carbon content (<0.03 wt%).

Before the tests, the specimens were polished using SiC paper, mirror-finished (3 μm), degreased in ethanol solution, and passivated in 10.5 wt% nitric acid solution during 15–20 h at room temperature.

2.2. Formation of passive films

The formation of the passive film was carried out by anodic polarization at a constant potential in nitric acid solution (40.5 wt%) at 50 °C for 120 min.

The stainless steels were polarized at three different potentials:

- 0.40 V/SSE, corresponding to a passive state;
- 0.55 V/SSE, corresponding to the beginning of a transpassive state;
- 0.70 V/SSE, corresponding to a transpassive state.

The anodic polarizations were conducted in a three-electrode cell. The potential was measured with respect to a saturated mercurous sulfate electrode (SSE), and Pt was used as a counter electrode.

2.3. XPS Analyses

After the different exposures, XPS analyses were performed with a VG ESCALAB 220i-XL spectrometer with Mg Kα X-ray source. Binding energies were corrected for

Table 1
Chemical composition of stainless steels

		Fe	Cr	Ni	Si	C	Mn	Mo	P	S
AISI 304L	(wt%)	69.09	18.46	10.21	0.39	0.017	1.48	0.36	0.024	0.001
	(at.%)	68.2	19.6	9.6	0.8					
Uranus S1N	(wt%)	61.23	17.72	15.05	4.03	0.007	1.88	0.067	0.016	<0.001
	(at.%)	58.5	18.2	13.7	7.7					

charge effects by taking the C 1s energy at 285.0 eV. The main parameters used to decompose detailed XPS spectra (Cr 2p 3/2, Ni 2p 3/2, Fe 2p 3/2 and Si 2p) are summed up in Table 2.

3. Results and discussion

3.1. Initial composition of passive films

Before anodic polarizations, XPS analyses were performed on the passivated specimen (10.5 wt% HNO_3 passivation). The composition of the passive films is shown in Fig. 1.

For both steels, the main compound of the passive layer is chromium. The passive layer is also composed of iron (23% for 304L and 13% for Uranus S1N) and in the case of Uranus S1N, of silicon. Although there is only 7% of silicon in the Uranus S1N matrix, there is 36% of this element in the passive layer of this steel. Ni is not identified in the passive films. It is interesting to notice that the Fe/Cr ratio is the same for Uranus S1N and 304L (≈0.26).

For both steels, the species in the passive layer have the same oxidation states: chromium is mainly as Cr(III) (Cr_2O_3 or $Cr(OH)_3$), iron is present as Fe(II) and Fe(III). The chemical form of silicon will be discussed later.

XPS depth profiles for the passive film formed on the stainless steels after nitric passivation (10 wt%) were

Table 2
Parameters used for deconvolution of XPS spectra (Avantage Software)

	Nickel			Iron			Chromium	
	Ni^0	NiO	$Ni(OH)_2$	Fe^0	Fe^{II}	Fe^{III}	Cr^0	Cr_2O_3
Binding energy (eV)	852.5	853.4	855.7	706.7	709.3	710.9	573.9	576.2
FWHM (eV)	1.3	1.4	2.3	1.2	3.1	2.4	1.7	2.2
	Chromium		Silicium 2p		Silicate		SiO_2	
	CrO_3	$Cr(OH)_3$	Si $2p^1/_2$	Si $2p^3/_2$	Si $2p^1/_2$	Si $2p^3/_2$	Si $2p^1/_2$	Si $2p^3/_2$
Binding energy (eV)	578.2	577.0	99.6	99.0	102.1	101.4	1.404	103.5
FWHM (eV)	2.1	2.2	0.9	0.9	1.5	1.4	1.1	1.0

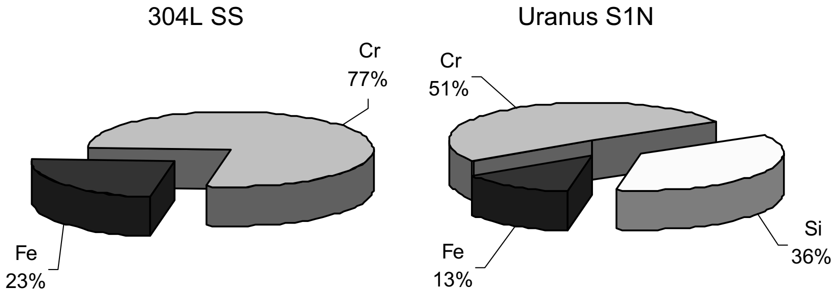

Fig. 1. Composition of passive films (at.%) after 10.5 wt% HNO_3 passivation.

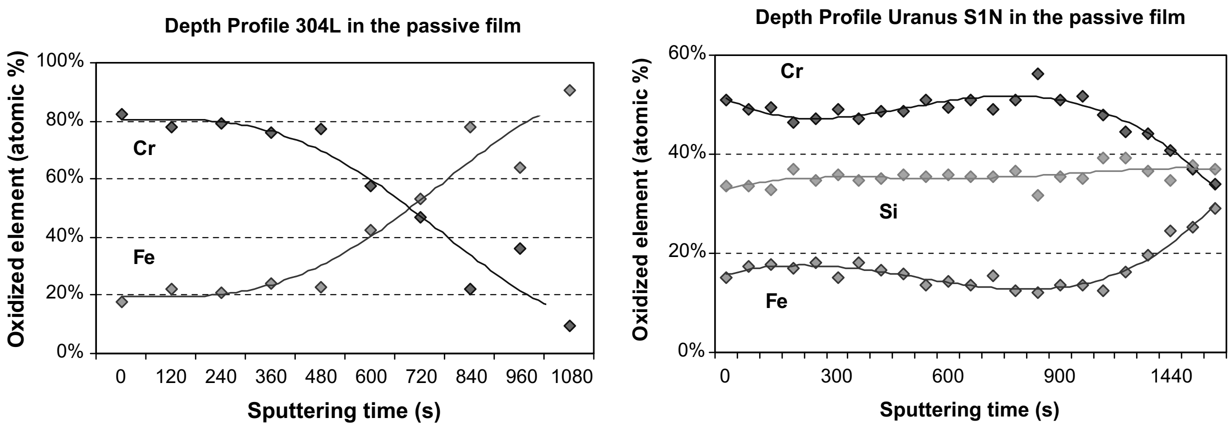

Fig. 2. Depth profiles for the passive film formed on 304L and Uranus S1N stainless steels by passivation in nitric acid solution (10.5 wt%) at room temperature.

performed by Ar^+ sputtering beam. As shown in Fig. 2, the Cr profile decreases as the sputtering time increases, whereas the reverse tendency is observed for the Fe profile. This evolution is the same for both steels. For Uranus S1N, the Si content is approximatively constant in the depth direction.

These observations suggest that Cr concentrated in the surface layer of the passive film and Fe concentrated in the inner layer. These results are in agreement with those of Honda and Kajimura [5,10] about the distribution of chromium and iron in the passive film. However, according to these authors, for a high Si-containing steel, the top surface film is enriched with Cr and the underneath film enriched with Si. By our XPS analyses, the concentration of Si at the metal–film interface is not confirmed in the rich Si steel (Uranus S1N).

3.2. Chemical form of silicon

The literature is not very clear concerning the chemical form of silicon in the passive layers of Si-containing stainless steels. Some authors assume a binary oxide is formed SiO_2–Cr_2O_3 [5] whereas others claim it is SiO_2 [13]. To clarify this, XPS spectra of a silicon wafer (SiO_2 on the top of metallic silicon) and a silicate (iron silicate) were performed. Binding energy of SiO_2 is 103.5 eV [14,15] whereas the silicon present in passive layer of Uranus S1N has a binding energy of 101.9 eV, the same as the one of silicate (see spectrum Fig. 3).

It will be pointed out that silicon is present as silicate and not as silicon oxide in the passive layers of Uranus S1N. The exact nature of this silicate has still to be determined. It is not purely an iron silicate, as the stoichiometry is not respected (twice more silicon that of iron). The nature of the silicate cannot be easily determined: it could be either a chromium silicate, or an iron–chromium silicate.

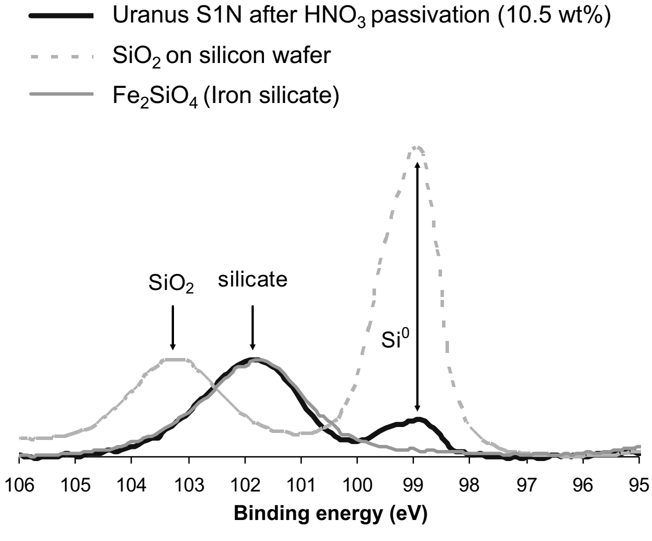

Fig. 3. Normalized XPS Spectra of Si 2p.

In the depth profile performed on Uranus S1N after passivation in nitric acid, silicon content in the passive layer is constant whereas chromium content decreases from surface to metal. This tends to prove that it is not a pure chromium silicate. In light of these results, it can be suggested a mixed silicate (chromium–iron). Further analyses are necessary to tell more on this subject.

3.3. Composition of the passive films after polarization

To simulate the oxidizing capacity of the medium, the stainless steels were polarized at three different potentials (0.40, 0.55 and 0.70 V/SSE) respectively corresponding to the passive, beginning of transpassive and transpassive state of the steels. The polarization curves of stainless steels in 40.5 wt% nitric acid at 50 °C are shown in Fig. 4. The compositions of the oxidized elements in the passive films after polarization are shown in Figs. 5 and 6, respectively for the 304L and Uranus S1N steel.

For both steels, the passive layers formed after polarization at 0.40 V/SSE (passive state) contain less iron (<10%) than the initial passive layers and therefore more chromium and more silicon. Polarizing a steel in its passive state leads to the iron dissolution which is contained in its passive layer, that is in agreement with the selective dissolution of iron during the passivation of alloys [6]. The species have the same oxidation states than for the HNO_3 passivation treated steels: Cr (III), Fe (II) and Fe (III), Si as silicate.

At the beginning of the transpassive state (0.55 V/SSE), the iron content remains very weak (<10%) for both steels. Iron is mainly present at the oxidation state III and chromium is always at the oxidation state III. The composition of the 304L passive film is the same as the one after polarization at 0.40 V/SSE, whereas the Uranus S1N has more silicon in its passive layer (54% instead of 40%). This additional silicon is present as SiO_2 (silicate 44% and SiO_2 10%) and SiO_2 concentrated in the external layer of the passive film as shown in the XPS spectra after a surface sputtering

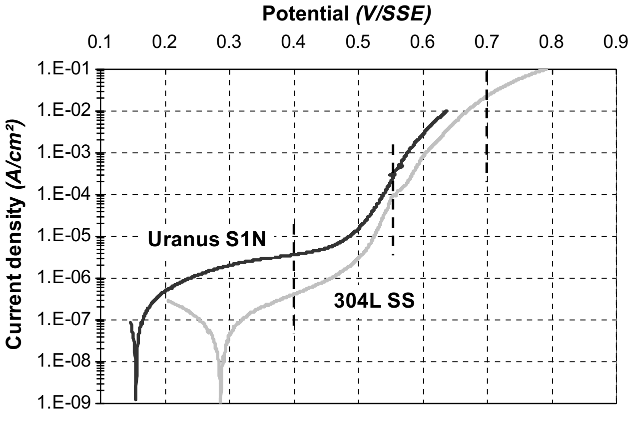

Fig. 4. Polarization curves of steels in nitric acid solution (40.5 wt%) at 50 °C.

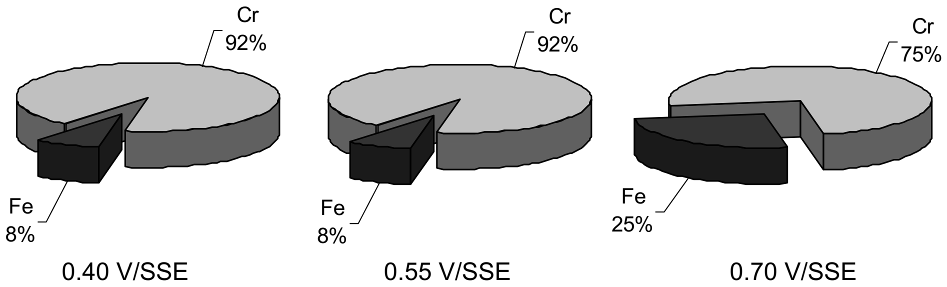

Fig. 5. Composition of the passive film (at.%) formed on 304L after polarization in nitric acid solution (40.5 wt%) at 50 °C.

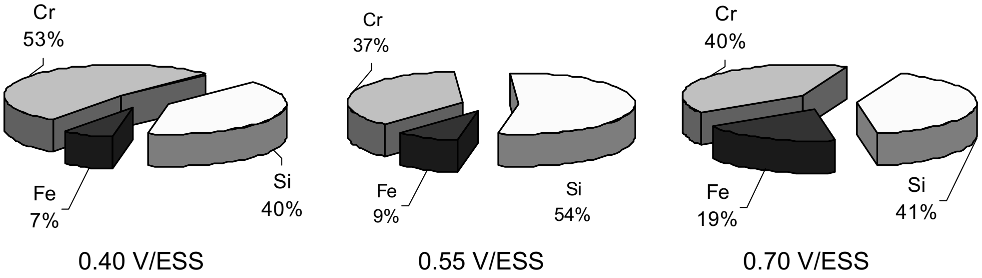

Fig. 6. Composition of the passive film (at.%) formed on Uranus S1N after polarization in nitric acid solution (40.5 wt%) at 50 °C.

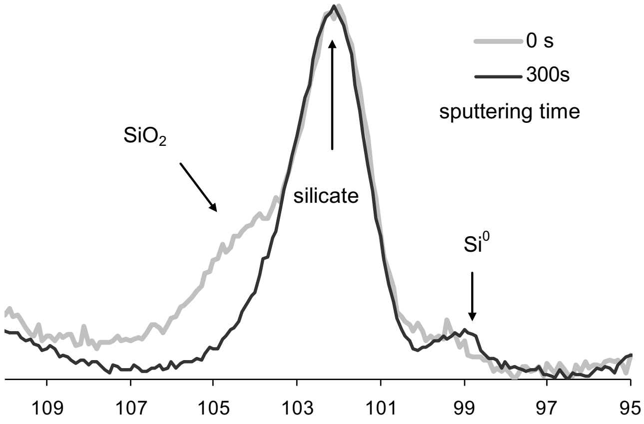

Fig. 7. Normalized XPS Spectra of Si 2p (Uranus S1N polarized at 0.55 V/SSE in nitric acid solution 40.5 wt% at 50 °C).

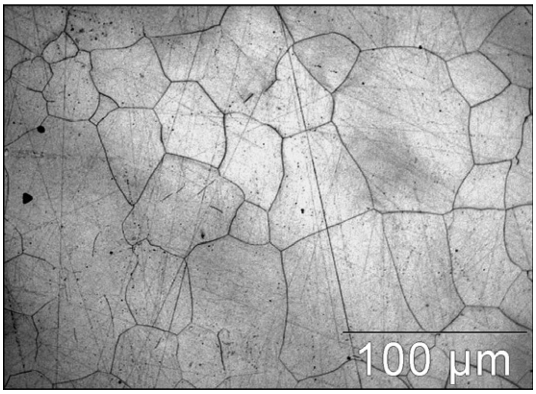

Fig. 8. Surface of the 304L after polarization at 0.55 V/SSE in nitric acid solution (40.5 wt%) at 50 °C.

(Fig. 7). These results are in agreement with other reported results [10,13].

When the steels are polarized in the far transpassive state (0.70 V/SSE), the passive layers change. In comparison with the passive films formed by polarization at 0.40 V/SSE, the films contain less chromium (and thus more iron). Iron is present at the oxidation state III, chromium at the oxidation state III, and silicon as a silicate. SiO_2 is not identified in the passive film. According to many authors [5,16], the decrease of chromium content in the passive film is due to the Cr_2O_3 dissolution as soluble Cr (VI) ions at this imposed potential.

As for the polarization in the transpassive domain (0.55 V/SSE and 0.70 V/SSE for 2 h), it is interesting to notice that 304L undergoes an intergranular corrosion (Fig. 8), whereas Uranus S1N exhibits a generalized corrosion.

The compositions of the passive film show that the silicon is present in a considerable amount and thus decreases the content of the other elements of the passive layer. Thereby, silicon just decreases the chromium content of the passive layer.

In the passive potential region, the presence of silicon is not benefic on the generalized corrosion rate. The passivation current density of the Uranus S1N is slightly higher than that of the 304L. The passive film of the Uranus S1N is less protective and so its generalized corrosion rate is higher than the one of 304L. These results are in agreement with those of the majority of the authors and with internal data. The Cr_2O_3 film is the most effective corrosion protective film to the dissolution of metal in a pure nitric acid media, and consequently, the impoverishment in chromium in the passive film leads to the reduction of the corrosion resistance.

In the transpassive potential region (0.55 V/SSE), the same tendency is noted. The silicon reduces the chromium content of the passive film. However, an additional form of silicon is present in the extreme surface: SiO_2. According to [5,7,10], the Si-oxide film inhibits the generalized corrosion by stifling the cathodic reaction, probably by reducing the electronic conductivity of the film or increasing the overpotential of the cathodic reaction. The effectiveness of Si on the resistance to generalized corrosion cannot be discussed starting from these results. In our experiments, the cathodic reaction does not occur on the material, but on the auxiliary electrode. Complementary examinations should be necessary to understand the role of SiO_2 in the generalized corrosion resistance.

3.4. Influence of silicon on the intergranular corrosion susceptibility

The intergranular corrosion is believed to result from the segregation of impurities at grain boundaries and the resultant formation of active sites on the surface [17]. So, the interactions between the surface and the electroactive components of the solution are not the same at the grain boundaries and grain faces: the electrochemical behavior of the grain boundaries and grain faces are different. Based on the hypothesis of Kasparova [11] (silicon induces changes in the electronic structure of admixture atoms), the addition of silicon in steels might lead to a modification of the polarization distribution on the surface.

To highlight differences of polarization distribution on the surface of the steels between the grain boundaries and grain faces, the following experiment was performed. Corrosion specimens of 304L and Uranus S1N were immersed in nitric acid in the presence of palladium (II) ions (HNO_3 40.5 wt%, at 80 °C). After corrosion testing (24 h), a palladium deposit was observed on the specimen surface. Its aspect corresponds to:

- a homogeneous repartition of Pd for the Uranus S1N;
- a Pd deposit more specifically into the gain boundaries for the 304L (Fig. 9).

The palladium (II) ions are reduced to Pd alongside the corrosion reaction of stainless steels. The palladium deposit would occur preferentially on the most active sites.

The deposition of palladium seems to indicate that the distribution of the polarization characteristics on the surface is different for high and low Si-containing stainless steels. In the case of the 304L, the selective deposition of palladium suggests that the cathodic reaction preferentially occurs at the grain boundaries, and consequently the dissolution of grain boundaries is faster than the one of the grain. This observation confirms the intergranular susceptibility of this steel in strongly oxidizing environment. On the other hand, in the case of Uranus S1N, the homogeneous repartition of palladium suggests that the cathodic reaction is not specifically catalyzed by the gain boundaries or faces, and consequently the polarization characteristics on the surface of the gain boundaries or grain faces are close. The silicon content and its distribution are probably the cause of this phenomenon.

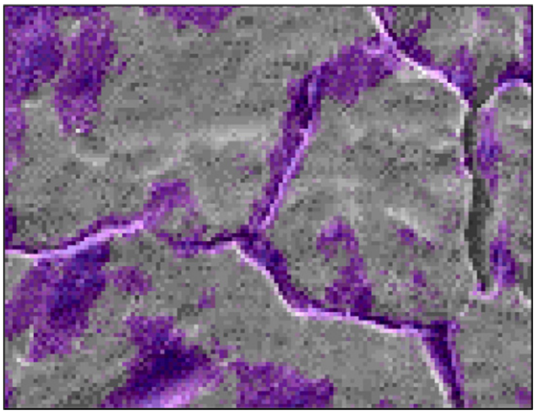

Fig. 9. SEM view of 304L and X-ray image of Pd (purple color) after immersion test in nitric acid solution containing Pd (II) ions (HNO_3 40.5 wt%, at 80 °C, for 24 h). (For interpretation of the references to color in this figure legend, the reader is referred to the web version of this article.)

Si concentration profiles across grain boundaries (−100 to +100 nm around grain boundaries) were performed by Honda [10], and the results have shown that the Si distribution is almost constant in the grain boundaries and faces for high Si-containing steels. From this result, the explanation of the similar electrochemical behavior of grain boundaries and faces may be connected with the homogeneous silicon distribution in the steel for the Uranus S1N.

4. Conclusion

The following conclusions may be drawn from the data presented in this preliminary work:

- Silicon is present in the passive layer in a considerable amount and thus decreases the content of each other element of the passive layer. Thereby, silicon just decreases the chromium content of the passive layer.
- In the passive potential region corresponding to an oxidizing media (pure HNO_3), the generalized corrosion rate of the high Si-containing austenitic stainless steel (Uranus S1N) is higher than that of the low Si-containing steel (304L). These results can be connected with the decrease of chromium content in the passive film.
- The chemical form of silicon in the passive films of Uranus S1N is mainly a silicate. An additional form of silicon, SiO_2, is noticed, but only under a potential inside the beginning of the transpassive state. Further analyses are necessary to determine which kind of silicate has been formed.

- In the transpassive potential region corresponding to a strongly oxidizing media (nitric acid containing oxidizing species), the presence of SiO_2 could explain the good corrosion resistance of high Si-containing austenitic stainless steels by decreasing the cathodic reaction rate.
- Differences of polarization distribution on the surface of the steels between the grain boundaries and grain faces have been highlighted. In the case of Uranus S1N, the cathodic reaction is not specifically catalyzed by the gain boundaries or faces, and consequently the polarization characteristics on the surface of the gain boundaries or grain faces are close.
- To better understand the relation between the intergranular corrosion susceptibility and the silicon distribution in the steels, further analyses of the composition of the grain boundaries and grain faces are necessary.

References

[1] K. Sugimoto, Bull. Jpn. Inst. Metals 24 (1985) 754.
[2] S. Haupt, H.H. Strehblow, Corros. Sci. 37 (1) (1995) 43.
[3] K. Asami, K. Hashimoto, S. Shimodaira, Corros. Sci. 18 (2) (1978) 151.
[4] H. Nagano, Corros. Eng. 37 (1988) 263.
[5] H. Kajimura, N. Usuki, H. Nagano, Electrochem. Soc. Proc. 97 (26) (1998) 332.
[6] K. Sugimoto, Corros. Eng. 53 (2004) 187.
[7] J.S. Armijo, B.E. Wilde, Corros. Sci. 8 (1968) 649.
[8] H. Coriou, A. Desestret, L. Grall, J. Hochmann, Corros. et Anticorros. 14 (4) (1966) 163.
[9] B.E. Wilde, Corros. Sci. 44 (10) (1988) 699.
[10] T. Honda, T. Yokosuka, Y. Arai, Corrosion NACE paper, 114, 1997.
[11] O.V. Kasparova, Protect. Metals 40 (5) (2004) 425.
[12] B. Ghiban, N. Ghiban, U.P.B. Sci. Bull. Series B 62 (3) (2000) 79.
[13] K. Hio, T. Adachi, T. Yamada, Y. Tsuchida, K. Nakajima, Y. Hosoi, Mater. Trans. 42 (8) (2001) 1723.
[14] A. Mosser, P. Humbert, Appl. Surf. Sci. 14 (83) (1983) 260.
[15] S. Suzuki, K. Yanagihara, S. Yamazaki, K. Tanaka, Y. Waseda, Surf. Interf. Anal. 35 (3) (2003) 276.
[16] M. Bojninov, G. Fabricius, P. Kinnunen, T. Laitinen, K. Mäkelä, T. Saario, G. Sundholm, Electrochem. Acta 45 (2000) 2791.
[17] M. Mayuzumi, J. Ohta, K. Kako, E. Kawakami, Corros. Sci. 56 (9) (2000) 910.